Upconversion fluorescence spectroscopy of Er^{3+}-doped lead oxyfluorosilicate glass

Shiqing Xu (徐时清), Zhongmin Yang (杨中民), Guonian Wang (汪国年),
Shixun Dai (戴世勋), Lili Hu (胡丽丽), and Zhonghong Jiang (姜中宏)

Shanghai Institute of Optics and Fine Mechanics, Chinese Academy of Sciences, Shanghai 201800

Upconversion fluorescence emission of Er^{3+}-doped oxyfluorosilicate glass excited at 975 nm is experimentally investigated. The results reveal that the intense green and red emission, and weak blue emission centered at 525, 543, 655, and 410 nm, respectively. A two-photon upconversion process is assigned to the green and red emission while a three-photon process is responsible for blue upconversion. The possible upconversion mechanisms are discussed based on excited state absorption and energy transfer between excited Er^{3+} ions. The intense upconversion fluorescence of Er^{3+}-doped lead oxyfluorosilicate glass may be a potentially useful material for developing upconversion optical devices.

OCIS codes: 160.4670, 160.4760, 160.2750, 160.2540, 170. 6280.

In recent years, considerable attention has been devoted to the conversion of near infrared radiation to visible light in rare-earth doped glass materials, for a wide range of applications, including color displays, optical data storage, biomedical diagnostics, sensors, undersea optical communications and upconversion lasers[1,2]. Many trivalent rare earth ions such as Er^{3+}, Tm^{3+}, Ho^{3+}, Pr^{3+} and Nd^{3+} were doped as absorption and emission centers in glass hosts. Among the rare-earth ions, Er^{3+} is the most popular as well as one of most efficient ions[3−6]. When a rare earth doped optical device is developed, the host material is a very important factor to be considered. So far, much effort has been spent on fluoride glasses owing to their lower phonon energy than oxide glasses. Unlike fluoride glasses, upconversion is seldom observed in oxide glasses with high phonon energies and can be limited to germanate[7,8], tellurite[9] and gallate[9] glasses that have comparatively low phonon energies. However, silicate glasses are the most chemically and mechanically stable and also are more easily fabricated into various shapes such as a rod and optical fiber[10]. Therefore, the design of a new silicate glass host for Er^{3+} to realize upconversion is a target at present.

Capobianco *et al.*[11] reported upconversion properties of Er^{3+} in lead silicate glasses, but it have only very faint upconversion fluorescence due to their large phonon energies. In this letter, we reported on the experimental investigation of upconversion fluorescence spectroscopy of new Er^{3+}-doped lead oxyfluorosilicate glass excited at 975 nm. The results show the generation of intense green and red emission and the weak blue emission centered around 525, 543, 655, and 410 nm, respectively. The possible upconversion processes and mechanisms involved excited state absorption and energy transfer between excited Er^{3+} ions are discussed.

The glass was prepared by mixing SiO$_2$, PbF$_2$ and Er$_2$O$_3$ powders in 50-g batches. SiO$_2$ and PbF$_2$ were common reagent grade. The Er^{3+} doping concentration in the glasses was 4.0 mol%, which was introduced as with 99.99% purity. The batch composition (mol%) of the glass host is 50SiO$_2$-50PbF$_2$. One undoped glass was prepared for measuring the Raman spectrum. The

mixtures were melted at $1000 - 1100°C$ for $30 - 50$ min in covered aluminum oxide crucibles in an electric furnace with N$_2$ atmosphere. After completely melting, the glass liquids were cast into a copper followed by annealing to room temperature. Then the glass was processed to a certain size for property testing. The upconversion luminescence spectrum was obtained with a TRIAX550 spectrofluorimeter upon excitation of 975-nm LD with a maximum power of 2 W. The Raman spectrum was recorded on a FT Raman spectrophotometer (Nicolet MODULE) within the range of $100-1200$ cm^{-1}. Nd:YAG operating at 1064 nm is used as the excitation source, and the laser power level was 500 mW. The infrared (IR) spectrum was recorded on a NIC Nicolet 740 FT IR spectrophotometer by KBr pellet technique. All the measurements were taken at room temperature.

The upconversion fluorescence spectrum in the visible wavelength range is shown in Fig. 1. Four emission bands centered at 410, 525, 543, and 655 nm, which correspond to the transitions $^2H_{9/2} \rightarrow {}^4I_{15/2}, {}^2H_{11/2} \rightarrow {}^4I_{15/2}, {}^4S_{3/2} \rightarrow {}^4I_{15/2}$, and $^4F_{9/2} \rightarrow {}^4I_{15/2}$, respectively, are simultaneously observed. Clearly, the blue emission
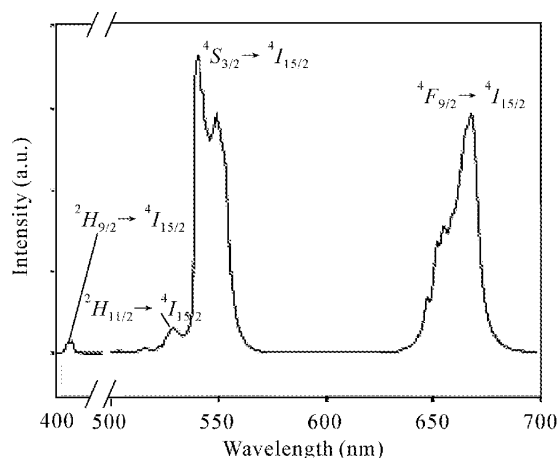

Fig. 1. Upconversion fluorescence spectrum of Er^{3+} doped lead oxyfluorosilicate glass.
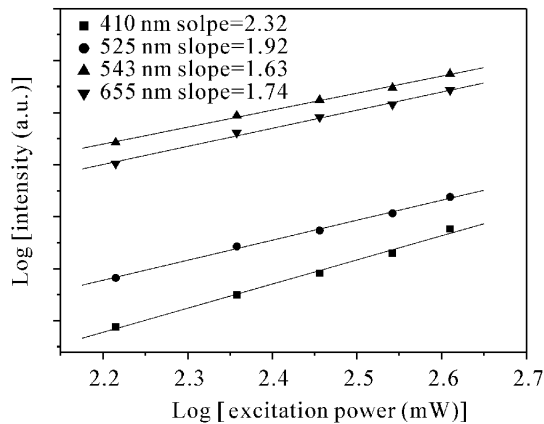
Fig. 2. Log-log plot of upconversion fluorescence emissions as a function of pump power at 975 nm.

at 410 nm is relative weaker than the green emission at 543 nm in Er^{3+}-doped lead oxyfluorosilicate glass.

The pump power dependence of the four upconversion fluorescence bands was analyzed and the results are depicted in the log-log plot of Fig. 2. As can be inferred from data, a two-photon upconversion process is assigned to the green and red emission from $^2H_{11/2}, ^4S_{3/2}$ and $^4F_{9/2}$ level, respectively, while a three-photon process is responsible for blue upconversion from $^2H_{9/2}$ level.

According to the energy matching conditions and the quadratic dependence on excitation power, the possible upconversion mechanisms for the emission bands are discussed based on the simplified energy levels of Er^{3+} presented in Fig. 3[12]. For the green emissions, in the first step, the $^4I_{11/2}$ level is directly excited at 975 nm. The second step involves the excitation processes based on the long-lived $^4I_{11/2}$ level as follows: energy transfer (ET) $^4I_{11/2}(Er^{3+})+^4I_{11/2}(Er^{3+}) \rightarrow ^4F_{7/2}$ $(Er^{3+})+^4I_{15/2}(Er^{3+})$, and excited state absorption (ESA) $^4I_{11/2}(Er^{3+})+$ a photon$\rightarrow ^4F_{7/2}(Er^{3+})$. The populated $Er^{3+}+^4F_{7/2}$ level then relaxes rapidly and nonradiatively to the next lower levels $^2H_{11/2}$ and $^4S_{3/2}$ resulting from the small energy gap between them. It is considered that the $^2H_{11/2}$ level is populated from $^4S_{3/2}$ by a fast thermal equilibrium between the levels[13]. The above processes then produce the two $^2H_{11/2} \rightarrow ^4I_{15/2}$ and $^4S_{3/2} \rightarrow ^4I_{15/2}$ green emissions centered at 525 and 543 nm, respectively. There exist two main possible pumping mechanisms for red emission in Er^{3+}-doped lead oxyfluorosilicate glass. The first pumping mechanism comprises the population of the $^4S_{3/2}$ level, by means of the process described previously, followed by a fast nonradiative decay through multiphonon interaction from the populated $^4S_{3/2}$ to $^4F_{9/2}$ and then to the $^4I_{15/2}$ ground state. In the other possible mechanism, the red emission at 655 nm is originated from the $^4F_{9/2} \rightarrow ^4I_{15/2}$ transition and the population of $^4F_{9/2}$ is based on the processes as follows: $^4I_{13/2}+$ a photon$\rightarrow ^4F_{9/2}$(ESA), and ET between Er^{3+} ions: $^4I_{13/2} + ^4I_{11/2} \rightarrow ^4I_{15/2} + ^4F_{9/2}$. The $^4I_{13/2}$ level is populated owing to the nonradiative relaxation from the upper $^4I_{11/2}$ level. For the blue emission, a possible mechanism is an energy transfer process called "cooperative upconversion"[14], in which two excited ions

at the $^4S_{3/2}$ level interact, and one is promoted to the $^4G_{11/2}$ level while second decays to the $^4I_{11/2}$ level. Another possible approach is the $^4F_{9/2} \rightarrow ^2H_{9/2}$ transition by absorption of a third pump photon. The populated $Er^{3+}+^4G_{11/2}$ level then relaxes rapidly and nonradiatively to the next lower levels $^2H_{9/2}$ resulting from the small energy gap between them. The transition probability involved in the above processes is small and the blue emission observed is weak.

Figure 4 shows the IR spectrum of Er^{3+} doped lead oxyfluorosilicate glass. A few bands in the region $463 - 1100$ cm^{-1} are assigned to stretching vibrations of F-Pb-F, $^-$O-Si-O$^-$ and Si-O-Si bonds at 463, 914 and 1050 cm^{-1}, respectively, and dissymmetry stretching vibration of $^-$O-Si-O$^-$ bond at 906 cm^{-1}. Figure 4 shows the Raman spectrum of an undoped $50SiO_2$-$50PbF_2$ glass, and the spectrum indicates the highest frequency phonon band is at 904 cm^{-1}. The Raman scattering peaks of Si-O-Si and $^-$O-Si-O$^-$ bonds are at 1060 and 950 cm^{-1}, respectively. But only one scattering peak at 904 cm^{-1} was found, which only can be dissymmetry stretching vibration of $^-$O-Si-O$^-$ bond in glass structure. The scattering peak moves to long wavelength, which can be that the intensity of $^-$O-Si-O$^-$ bond was weaken owing to polarization of Pb^{2+} and nonbridging oxygens.
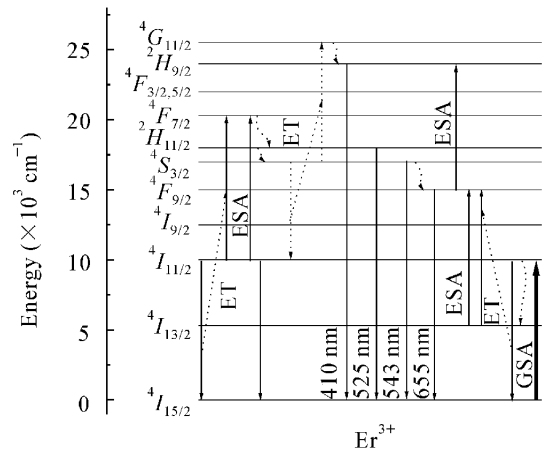

Fig. 3. Simplified energy level of Er^{3+} and possible transition pathways in Er^{3+} doped lead oxyfluorosilicate glass.
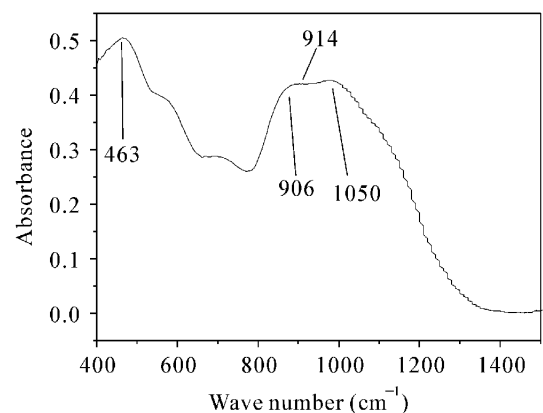

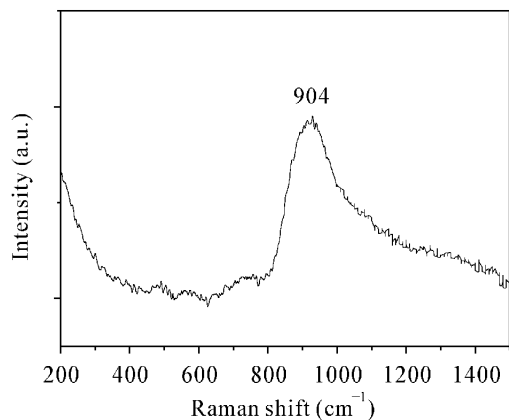Fig. 4. The IR spectrum of Er^{3+} doped lead oxyfluorosilicate glass.

Fig. 5. The Raman spectrum of undoped lead oxyfluorosilicate glass at room temperature.

Layne *et al.*[2] have discussed the multiphonon relaxation of rare-earth ions in oxide glasses. The approximate frequencies of the high-energy phonons in each glass are: borate: 1350 cm^{-1}, phosphate: 1100 cm^{-1}, silicate: 1000 cm^{-1}, germanate: 900 cm^{-1}, tellurite: 800 cm^{-1} and fluoride: $350 - 500 \text{ cm}^{-1}$[2,15] glasses. From the above result we can deduce that fluoride ions have an important influence on the formation of glass network. The lead fluoride added can enter the glass as a network former as well as network modifier, and increases the number of nonbridging oxygens in the glass network. The Er^{3+} ions in the glass are surrounded by nonbridging oxygens of SiO_4 tetrahedra and lead-fluoride polyhedra. The energy of local vibrational modes coupled to the Er^{3+} enters could be smaller than that of the maximum phonon energy of glass network[16]. Therefore, the multiphonon rate of Er^{3+} in lead oxyfluorosilicate glass is among lowest in above glasses systems except tellurite and fluoride glasses. Consequently, the upconversion fluorescence rate of Er^{3+} in lead oxyfluorosilicate glass could be the highest in the above glass systems except tellurite and fluoride glasses. In the spectral region studied, the $^4S_{3/2}$ level of Er^{3+} has the largest energy gap below (3010 cm^{-1}), and the brightest upconversion fluorescence is then expected from this level.

In conclusion, the high efficient IR to visible upconversion fluorescence of Er^{3+}-doped lead oxyfluorosilicate glass is investigated. The intense green and red emission, and weak blue emission centered at 525, 543, 655, and 410 nm, which correspond to the transitions $^2H_{11/2} \rightarrow {}^4I_{15/2}, {}^4S_{3/2} \rightarrow {}^4I_{15/2}, {}^4F_{9/2} \rightarrow {}^4I_{15/2}$, and $^2H_{9/2} \rightarrow {}^4I_{15/2}$, respectively. The results suggest that Er^{3+}-doped lead oxyfluorosilicate glass may be a potentially useful material for developing upconversion optical devices.

References

1. A. S. Oliverira, M. T. De Araujo, A. S. Gouveia-Neto, A. S. B. Sombra, J. A. Medeiros Neto, and N. Aranha, J. Appl. Phys. **83**, 604 (1998).
2. Z. Pan, S. H. Morgan, A. Loper, V. King, B. H. Long, and W. E. Collins, J. Appl. Phys. **77**, 4688 (1995), and references therein.
3. K. Soga, H. Inoue, and A. Makishima, J. Non-Cry. Solids **274**, 69 (2000).
4. H. Lin, E. Y. B. Pun, and X. R. Liu, J. Non-Cry. Solids **283**, 27 (2001).
5. H. Higuchi, M. Takahashi, Y. Kawamoto, K. Kadono, T. Ohtsuki, N. Peyghambarian, and N. Kitamura, J. Appl. Phys. **83**, 19 (1998).
6. M. Tsuda, K. Soga, H. Inoue, S. Inoue, and A. Makishima, J. Appl. Phys. **85**, 29 (1999).
7. Z. Pan, S. H. Morgan, K. Dyer, A. Ueda, and H. Liu, J. Appl. Phys. **79**, 8906 (1996).
8. H. Yamada and K. Kojima, J. Non-Cry. Solids **259**, 57 (1999).
9. S. Tanabe, K. Hirao, and N. Soga, J. Non-Cry. Solids **122**, 79 (1990).
10. S. Q. Xu, Z. M. Yang, S. X. Dai, J. H. Yang, L. L. Hu, and Z. H. Jiang, Chin. Phys. Lett. **20**, 905 (2003).
11. J. A. Capobianco, G. Prevost, P. P. Proulx, P. Kabro, and M. Bettinelli, Optical Materials **6**, 175 (1996).
12. H. Lin, G. Meredith, S. Jiang, X. Peng T. Luo, N. Peyghambarian, and E. Y. B. Pun, J. Appl. Phys. **93**, 186 (2003).
13. H. Berthou and C. K. Jorgensen, Opt. Lett. **15**, 1100 (1990).
14. P. Xie and S. C. Rand, J. Opt. Am. B **11**, 901 (1994).
15. S. Todorki, X. Kirao, and N. Soga, J. Non-Cry. Solids **143**, 46 (1992).
16. L. Huang, X. Liu, W. Xu, B. Chen, and J. Lin, J. Appl. Phys. **90**, 5550 (2001).